Impurity cyclotron resonance lines of barrier donor electrons in quantum wells

David M. Larsen and Herbert L. Fox
Physics Department, University of Massachusetts, Lowell, Massachusetts 01854
(Received 12 October 1999)

We have investigated by numerical simulation the zero-temperature line broadening of the cyclotron resonance transitions of a dilute system of randomly situated barrier donors, with centers consisting of positive donor ions fixed in the barrier region of a quantum well to which are bound electrons in the adjacent well. Inhomogeneous line shapes due to interdonor Coulomb interactions are obtained. Discussion is restricted to the case in which magnetic fields are sufficiently high that the electrons can be treated semiclassically (exchange can be neglected). The simulations indicate that a monolayer of donor ions produces a single highly asymmetric and relatively broad line, with the excitation induced by each absorbed photon being shared among a number of donors. However, if the same donor ions are distributed among several monolayers the absorption predicted is a finely spaced comb of well-resolved relatively narrow transition lines, each line deriving from a different monolayer. In this case the excitation induced by an individual absorbed photon is more localized. Parameters chosen for the simulation are realistic for GaAs-$Al_xGa_{1-x}As$ quantum wells.

I. INTRODUCTION

Although considerable magnetospectroscopic data on dilute systems of localized electrons in quantum wells exists in the literature, the problem of determining from first principles the spectral line shapes to be expected in such systems has been largely neglected. As an initial step in this direction we have investigated the intrinsic line broadening at zero temperature and high magnetic fields of a dilute two-dimensional system of quantum well electrons each of which is bound to a positively charged donor ion in a barrier adjacent to the well. These ions, equal in number to the electrons, are assumed to reside at random positions in planes located at discrete offset distances d from the center of the quantum well. When values of d are sufficiently small compared to the mean interelectron spacing, individual electrons can become bound to individual ions. At zero temperature each donor ion captures an electron, confining its wave function to a region of the plane of the quantum well (taken to be parallel to the x-y plane) near to that particular donor ion. These confined states are known as ''barrier donors.'' Spectral lines associated with barrier donors have been studied in magneto-optical experiments.[1–3] Barrier donors would seem to be excellent candidates for an initial theoretical study of impurity magneto-optical line shapes in quantum wells because in high magnetic fields and narrow quantum wells their electronic wave functions are so simple, consisting to a very good approximation simply of a product of a free-electron wave function in a magnetic field and the ground-state subband wave function. Moreover, because the energy of the strong transition line of a barrier donor is sensitive to the offset of the donor ion from the quantum well, measurements of line shapes of barrier donors present in physical samples could in principle be used to study the variation of concentration of the donor ions along the z direction. Success in such an endeavor would depend upon a theoretical understanding of the line shapes.

Unlike shallow donors in bulk semiconductors, barrier donors have both permanent dipole and quadrupole moments. These give rise to spatially fluctuating electric fields and electric-field gradients in the quantum well, which, in turn, perturb the donors, creating fluctuations in donor transition energies and therefore inhomogeneous broadening of the donor line. A second, and, for monolayers, a much more important source of line broadening at low impurity densities is the resonant van der Waals interaction between donors,[4] whereby an excited donor can transfer its excitation, via electron-electron interaction, to a donor initially in the ground state. This process produces excited eigenstates that consist of clusters of excited donors with energies that are shifted by varying amounts from the unperturbed donor absorption energy.

To focus on the essentials of the interacting barrier donor problem we assume that there is only one quantum well present, which is sufficiently narrow that the electrons can be considered to be confined to a plane, taken as the x-y plane. We define the ''donor center'' of a barrier donor to be the projection of the donor ion on the x-y plane. (The ''donor center'' of a barrier donor is so called because the electronic charge distribution associated with each eigenstate of an isolated barrier donor is cylindrically symmetric about that point.)

The high magnetic field behavior of this model is governed by the interplay of the following lengths: (a) the cyclotron radius r_c, which determines the size of the electronic wave function, (b) the separation of nearby donor centers r_{sep}, which increases as the number of donor ions per unit area n decreases, and (c) the offset distances of the planes occupied by the donor ions from the x-y plane, designated d_i (or just d for monolayers). The lengths r_c and r_{sep} are defined in this paper by

$$r_c=(\hbar/m\omega_c)^{1/2}, \tag{1}$$

where m is the band mass of the electron in the quantum well and ω_c is its cyclotron frequency defined by $\omega_c=eB/mc$, where B is the applied magnetic field, and

$$r_{\mathrm{sep}}=n^{-1/2}. \tag{2}$$

In our simulations the donor ions occupy either a single monolayer or, alternatively, a number of adjacent monolayers separated by 0.28 nm and contained within a slab of thickness much smaller than $r_{\rm sep}$. (The donor centers, on the other hand, are permitted to occupy any position within the confines of the circular boundary delimiting the donor system under consideration.) The separation chosen is one-half of a lattice constant in GaAs.

The present study deals with cases for which $r_c \ll r_{\rm sep}$ (where exchange effects can be neglected) and donor offsets are not much larger than $0.2r_{\rm sep}$; for offsets greater than about $0.5r_{\rm sep}$ our simulations show that the electron equilibrium positions start to become strongly affected by electron-electron interaction to the extent that these positions become only weakly correlated with the donor centers. (For offsets greater than $r_{\rm sep}$ the electrons form a latticelike structure, largely uncorrelated with the donor center positions.)

In Sec. II we discuss pertinent properties of the ground state and relevant excited states of isolated barrier donors. We next consider absorption line broadening of a monolayer of interacting barrier donors in the low-density limit. Finally we discuss line broadening of barrier donor systems at experimentally interesting densities and high magnetic fields for the GaAs-$Al_xGa_{1-x}As$ quantum well both for single monolayers (delta doping) and uniformly doped thin slabs.

II. ISOLATED BARRIER DONORS

The Hamiltonian for the electron belonging to the jth barrier donor in a magnetic field can be written in the form

$$H_{\rm BD}(j) = H_0(j) - 2/(\rho_j^2 + d_j^2)^{1/2}, \tag{3}$$

where, in the symmetric gauge

$$H_0(j) = -\nabla_j^2 + \frac{\gamma}{i}\frac{\partial}{\partial \phi_j} + \frac{1}{4}\gamma^2\rho_j^2. \tag{4}$$

Both Eqs. (3) and (4) are written in cylindrical coordinates and donor atomic units wherein lengths are in units of the bulk donor Bohr radius a and energies are in units of the bulk donor Rydberg constant R. The bulk semiconductor referred to is the well semiconductor. (For GaAs, $a = 10\,{\rm nm}$ and $R = 46.2\,{\rm cm}^{-1}$.) The donor center of barrier donor j is taken to be at the origin in these equations. The dimensionless magnetic field γ is defined in the usual way

$$\gamma = a^2/r_c^2 = \hbar\omega_c/2R, \tag{5}$$

and d_j is the offset of the donor ion j from the x-y plane. The coordinate ρ_j is the distance of the electron that is bound to barrier donor j from the center of that donor. Note that for GaAs the magnetic field in teslas, B, is related to γ by

$$B = 6.56\gamma.$$

For the strong magnetic fields and offsets considered here it is permissible to approximate the donor eigenstates by free-particle Landau level wave functions $\psi_{N,M}$, where N and M are, respectively, the Landau level and z-angular momentum quantum number. The ground-state donor wave function in this approximation is the most compact of the lowest-lying free-particle Landau level wave functions ($N = 0$, $M = 0$) and has the form

$$\psi_{N,M}(\rho_j) = \psi_{0,0}(\rho_j) = (\gamma/2\pi)^{1/2}\exp(-\gamma\rho_j^2/4). \tag{6}$$

Notice that as $\gamma \to \infty$ this wave function collapses to a point charge located at the classical electrostatic equilibrium position, the donor center. We are interested in optical transitions from $\psi_{0,0}$ to excited states lying above the ground state by approximately $\hbar\omega_c$ (or, in donor atomic units, 2γ.) There exists only one such free-electron state that can be reached by a dipole transition from $\psi_{0,0}$, and that is $\psi_{1,1}$, given by

$$\psi_{1,1}(\boldsymbol{\rho}_j) = (\gamma/2\pi^{1/2})\rho_j e^{i\phi_j}\exp(-\gamma\rho_j^2/4). \tag{7}$$

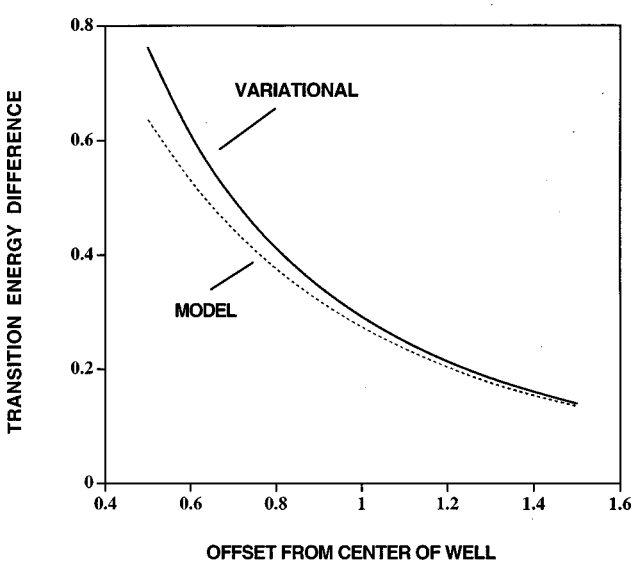

FIG. 1. Difference between the barrier donor and free-particle cyclotron resonance energies at $\gamma = 2$ (the barrier donor always has the higher energy). The dashed line represents calculations based on the two-dimensional model of the present paper; the solid line represents a variational calculation for a quantum well of thickness 10 nm. Offset distances and energies are in donor atomic units (a and R, respectively).

Of particular interest is the sensitivity of the donor transition energy to the offset of the donor ion from the x-y plane. The dashed line in Fig. 1 shows the difference between the donor and free-particle cyclotron transition energies for the present model (wave functions $\psi_{0,0}$ and $\psi_{1,1}$ for the ground and excited states, respectively, and the electron confined to the x-y plane) at a particular fixed magnetic field ($\gamma = 2$) and varying offset distances. The solid line shows a more realistic calculation in which is assumed a GaAs quantum well that is 10 nm (one bulk donor Bohr radius) wide and enclosed by infinitely high barriers. The ground and excited states are variational approximations found by replacing $\exp(-\gamma\rho_j^2/4)$ in Eqs. (6) and (7) by trial functions $\exp(-H\rho_j^2/4)\exp[-\kappa(\rho_j^2+\delta^2)^{1/2}]\cos(\pi z)$, normalizing and minimizing the expectation value of the energy in each state with respect to the three parameters H, κ, and δ. As is to be expected, the present model and the variational model approach each other as the offset from the center of the well (or the offset from the x-y plane in the present model) increases.

In a later discussion use will be made of the fact, apparent in Fig. 1, that for each offset the magnitude of the derivative of the model curve is always less than that of the variational curve.

As a check on the validity of our use of single free-particle Landau functions we expanded the exact ground-state eigenfunction in Landau level wave functions for a GaAs quantum well 10 nm in width with infinitely high barriers.[5] Using a fixed (and typical) offset of 15 nm between the donor ion and the well center we estimated the squared amplitude of $\psi_{0,0}$ in the exact wave function to be 0.967 at $\gamma=0.5$, 0.993 at $\gamma=1.0$, and 0.999 at $\gamma=2.0$. A similar calculation for $\psi_{1,1}$ in the excited state yields 0.935 at $\gamma=0.5$, 0.984 at $\gamma=1.0$, and 0.997 at $\gamma=2.0$. These results support the use of single free-electron wave functions in the range of fields and offsets of interest.

The donors perturb each other by producing weak in-plane electric fields. As a result each donor electron will find itself subject to a weak electric field. We shall treat this perturbation variationally by assuming that the effect of this field is to displace the center of symmetry of the donor electron wave function to a new ''equilibrium'' position away from the donor center.

Without loss of generality we can suppose that donor electron j is subjected to a weak uniform electric field in the negative x direction E_x. Then

$$H(j)=H_{\mathrm{BD}}(j)-Fx, \tag{8}$$

where F is the dimensionless electric force in the positive x direction, given by

$$F=|eE_x|a/R.$$

Here E_x is to be evaluated at the donor center. We introduce the ground-state trial function

$$\psi_{0,0}(x_j,y_j,x_0)=(\gamma/2\pi)^{1/2}\exp(-i\gamma x_0 y_j)\times\exp\{-\gamma[(x_j-x_0)^2+y_j^2]/2\}, \tag{9}$$

which is the same wave function as in Eq. (6) but with the center of symmetry of its associated charge distribution shifted a distance x_0 in the positive x direction. Treating x_0 as a variational parameter we minimize the expectation value of $H(j)$ of Eq. (8) in the wave function of Eq. (9). This leads to the equation

$$-F=(\gamma/2\pi)\int_{-\infty}^{\infty}dy_j\int_{-\infty}^{\infty}dx_j\exp\{-\gamma[(x_j^2+y_j^2)]/2\}\times\{-2(x_j+x_0)/[(x_j+x_0)^2+y_j^2+d_j^2]^{3/2}\}. \tag{10}$$

The right-hand side of Eq. (10) is simply the classical electrostatic force exerted on the electronic charge distribution of the jth electron by donor ion j, whereas F is the force exerted on the electron by the uniform field. Thus Eq. (10) states that the center of symmetry of the electronic charge distribution occupies a point where the electron is in classical electrostatic equilibrium. Under circumstances in which $d_j \ll r_{\mathrm{sep}}$ as assumed in this paper, it is permissible to set to set F equal to zero (see Appendix A). In that case x_0, being proportional to F for F small, is also zero.[6]

III. LOW-DENSITY LIMIT—MONOLAYERS

In the low-density limit we are interested in those terms in the donor-donor interaction Hamiltonian H_c, whose effect on the donor transition energies falls off least rapidly with the separation between donors. Such terms must become dominant as the donor separations become larger and larger. Let the centers of symmetry of the wave functions of electrons belonging to donors i and j occupy the electrostatic equilibrium positions that would be assumed by classical point electrons. (In the case of low donor density considered here, these are, to a sufficient approximation, the respective donor centers.) We denote the displacement of the center of symmetry of the wave function of donor electron i from that of donor electron j by $\mathbf{s}_{ij}$ and the separation of donor center i from the center of symmetry of the wave function of electron j by $\mathbf{S}_{ij}$. Then the Coulomb interaction between donors has the form

$$H_C(i,j)=2/|\mathbf{s}_{ij}+\boldsymbol{\rho}_i-\boldsymbol{\rho}_j|-2/(|\mathbf{S}_{ij}-\boldsymbol{\rho}_j|^2+d_i^2)^{1/2}-2/(|\mathbf{S}_{ji}-\boldsymbol{\rho}_i|^2+d_j^2)^{1/2}, \tag{11}$$

where $\boldsymbol{\rho}_j$ is the displacement of electron j from the position of the center of symmetry of its wave function. In our low-density approximation

$$\mathbf{s}_{ij}=\mathbf{S}_{ij}=\mathbf{S}_{ji}. \tag{12}$$

For a monolayer $d_i=d_j=d$ in Eq. (11).

If Eq. (11) is expanded for d and ρ values very small compared to s_{ij} the leading terms affecting the transition energy turn out to be $H_{VW}(i,j)$ given by

$$H_{VW}(i,j)=2\boldsymbol{\rho}_i\cdot\boldsymbol{\rho}_j/s_{ij}^3-6(\mathbf{s}_{ij}\cdot\boldsymbol{\rho}_i)(\mathbf{s}_{ij}\cdot\boldsymbol{\rho}_j)/s_{ij}^5. \tag{13}$$

The complete two-donor Hamiltonian in this approximation is

$$H_{\mathrm{BD}}(i)+H_{\mathrm{BD}}(j)+H_{VW}(i,j). \tag{14}$$

It is instructive to investigate the effect of H_{VW} on the cyclotron transition of a two-donor system where both donors have the same offset distance d. The ground state of the unperturbed system is

$$\psi_{0,0}(\rho_i)\psi_{0,0}(\rho_j), \tag{15}$$

a state whose unperturbed energy we take to be zero and that is connected by the dipole matrix element for optical absorption to the state

$$[\psi_{1,1}(\rho_i)\psi_{0,0}(\rho_j)+\psi_{0,0}(\rho_i)\psi_{1,1}(\rho_j)]/\sqrt{2} \tag{16}$$

with unperturbed energy equal to $E_{\mathrm{unp}}(d)$. (The wave function of Eq. (16) is one of two excited eigenstates involving $\psi_{1,1}$ and $\psi_{0,0}$ of the Hamiltonian in Eq. (14). The other eigenstate $[\psi_{1,1}(\rho_i)\psi_{0,0}(\rho_j)-\psi_{0,0}(\rho_i)\psi_{1,1}(\rho_j)]/\sqrt{2}$, has zero oscillator strength because it is antisymmetric upon the interchange $i\leftrightarrow j$.) The perturbation, $H_{VW}(i,j)$ affects the ground-state energy only in second order, an effect that is negligible in the low-density limit, as explained in Appendix A. However, the excited state energy is affected in first order and has a perturbed energy equal to

$$E_{\mathrm{unp}}(d)-1/\gamma s_{ij}^3, \tag{17}$$

which follows from

$$\langle \psi_{1,1}(\rho_i)\psi_{0,0}(\rho_j)|H_{VW}(i,j)|\psi_{0,0}(\rho_i)\psi_{1,1}(\rho_j)\rangle = -1/\gamma s_{ij}^3. \tag{18}$$

The generalization of this argument to the calculation of the spectrum of an N-donor system in a monolayer is straightforward. The N-donor ground-state Φ_{GS} is

$$\Phi_{GS} = \prod_{j=1}^{N} \psi_{0,0}(\rho_j). \tag{19}$$

This state is unaffected to lowest order by $H_{VW}(i,j)$ (see Appendix A). States for which only one donor is excited form a particularly simple N-dimensional orthonormal basis set for excited states reached from the ground state by absorption of a single photon in a dipole transition. These have the form

$$\Psi_k = \psi_{1,1}(\rho_k)\prod_{j\neq k}^{N} \psi_{0,0}(\rho_j), \quad 1 \leqslant k \leqslant N \tag{20}$$

and have a common unperturbed energy $E_{unp}(d)$. This degeneracy is broken by $H_{VW}(i,j)$ leading to N excited eigenstates Φ_l, with various excitation energies. Each eigenstate has a probability of excitation from the ground state via a dipole transition that is proportional to[7]

$$\left| \left\langle \sum_{k=1}^{N} \Psi_k \middle| \Phi_l \right\rangle \right|^2. \tag{21}$$

We have constructed a computer realization of this model by placing N donor ions at random positions within a disk that is parallel to the x-y plane and that resides inside the barrier at offset d from that plane. Using Eq. (18) we construct the matrix H_{ij} according to

$$H_{ij} = -1/\gamma s_{ij}^3 \quad (i \neq j) \quad \text{and} \quad H_{ii} = E_{unp}(d). \tag{22}$$

All eigenvalues of H_{ij} and their corresponding eigenvectors are calculated. An unweighted histogram of energies is plotted to find the density of transition energies. A second histogram of energies is constructed for the line-shape simulation but for this histogram each energy is weighted according to the square of the transition dipole moment [Eq. (21)] of its corresponding eigenfunction. The process is then repeated until sufficiently smooth histograms are generated. Plots that are independent of all parameters in the problem (n, d, and γ) are obtained by setting the unperturbed transition energy $E_{unp}(d)$ equal to zero, measuring distances s_{ij} in Eq. (22) in units of r_{sep} and energies in donor density units, i.e., units of

$$(na^2)^{3/2}R/\gamma.$$

All histograms are normalized to unit area for the energy range from $-\infty$ to ∞. We seek to approximate the line shape and density of transition energies for an effectively infinite number of donors by using samples with values of N no greater than 800.

The sharply peaked lines in Fig. 2 represent the results for the density of transition energies for $N=400$ (diamond symbols) and $N=800$ (dashed line). Also shown in Fig. 2 for comparison (solid line) is a predicted absorption line shape

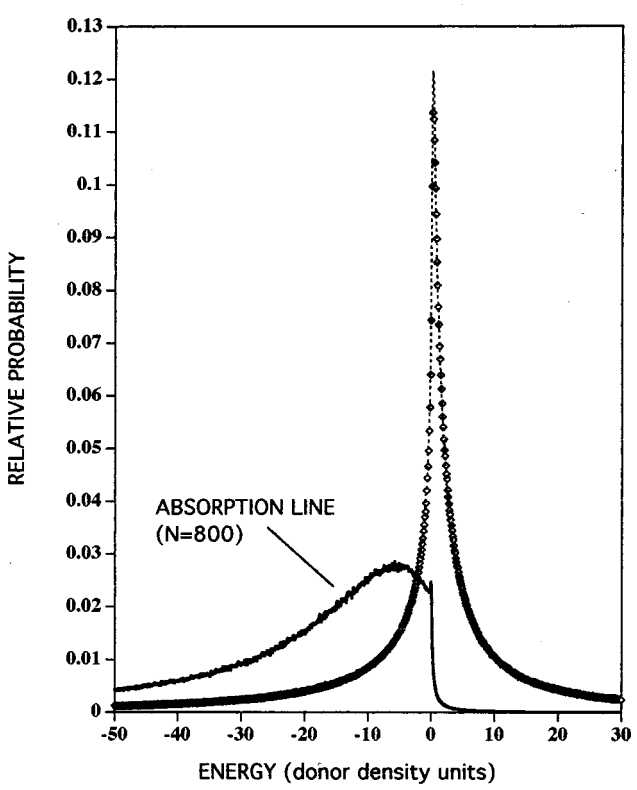

FIG. 2. Comparison of predicted absorption line shape for a monolayer in the extreme low-density limit with the unweighted transition energy density spectrum, this latter calculated for $N=400$ (diamond symbols) and $N=800$ (dashed interpolated line). The zero of energy is the transition energy of an isolated barrier donor.

for this system calculated using $N=800$. Clearly evident is the remarkable effect of the weighting by oscillator strength. The fact that the off-diagonal matrix elements of H_{ij} are, from Eq. (18), *negative*, results in suppression of the positive-energy part of the density of transition energies line and enhancement of the low-energy tail of that line.

The eigenstates of H_{ij} are linear combinations of the basis states Ψ_k defined in Eq. (20). Physically this means that the excitation created by the absorption of a photon is not localized on a single donor but is shared among the donors. Of considerable interest is the extent to which such an excitation is spread out in space. We have examined this problem by defining, for each eigenvector Φ_i of our Hamiltonian matrix, the position of the ''center'' of the excitation associated with Φ_i and the ''radius'' of that excitation. We expand Φ_i in our excited basis functions according to

$$\Phi_i = \sum_{k=1}^{N} c_{ik}\Psi_k, \tag{23}$$

then define the ''center'' of the excitation by

$$\mathbf{r}_i^{(C)} = \sum_{k=1}^{N} \mathbf{r}_k |c_{ik}|^2 \tag{24}$$

and its ''radius'' by

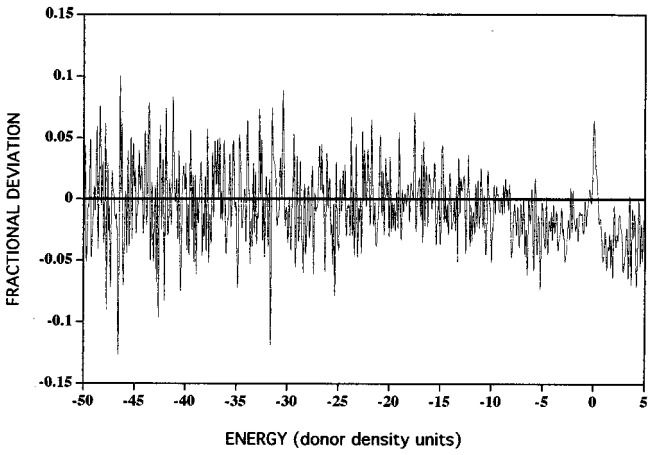

FIG. 3. Fractional deviation of the monolayer absorption histogram calculated with $N=400$ from that calculated with $N=800$.

$$R_i=\left[2\sum_{k=1}^{N}|\mathbf{r}_k-\mathbf{r}_i^{(C)}|^2|c_{ik}|^2\right]^{1/2}, \tag{25}$$

where $\mathbf{r}_k$ is the displacement of the center of donor k from the center of the disk containing all of the donors.

Eigenvectors with energies close to zero turn out to have a relatively high probability of representing large-radius excitations. A certain (small) percentage of these excitations can have radii that are comparable to the radius of the donor sample even for samples as large as the largest considered in this paper ($N=800$). Energies and oscillator strengths calculated for such excitations should be relatively strongly affected by the sample boundary. As a result we do not find very good convergence of the line shape near $E=0$ with increasing N.

To ameliorate this problem we have chosen not to accept contributions to our calculated line shapes from eigenfunctions likely to have been affected by the boundary. We attempt to achieve this by dividing the disk that contains all the donors into two parts, a smaller concentric disk that we call the ''inner disk'' and the remaining outer annulus. We accept contributions from only those wave functions Φ_i for which the center of the associated excitation lies within the inner disk and for which

$$r_i^{(C)}+R_i<R_{\text{disk}}, \tag{26}$$

where R_{disk} is the radius of the disk containing all the donors. For the calculations reported in this paper we have taken the area of the inner disk to be half that of the disk containing all the donors.

It is clear that as N goes to infinity this procedure will converge to the exact line shape. What is less clear is how closely the line shape found at $N=800$ approximates the exact line shape. Line shapes calculated for $N=400$ are so close to those for $N=800$ that it is difficult to distinguish them in the statistical noise of our calculations. In Fig. 3 we display the difference between these line-shape histograms by subtracting ordinates of the $N=400$ histogram from those of the $N=800$ histogram and dividing this difference by the ordinate of the $N=800$ histogram at each energy. Adjacent points so obtained are connected to form the oscillating curve in Fig. 3. Small deviations between the line-shape curves are apparent between energies of -10 and $+5$. The histogram in Fig. 3 is calculated from 82 400 realizations for $N=400$ and 19 600 realizations for $N=800$. The absorption line-shape curve in Fig. 2 represents results for 19 200 realizations. In both of these figures the width of the energy boxes for the histograms is 0.1. [The energy scale is in donor density units; to convert into units of R, values of the abscissa should be multiplied by $(na^2)^{3/2}/\gamma$.] Small but statistically significant differences appear in the energy range between -10 and $+5$. The close agreement between the $N=400$ and $N=800$ calculations suggests, but does not prove, that the absorption line shape shown in Fig. 2 may approximate well the line shape for infinite N.

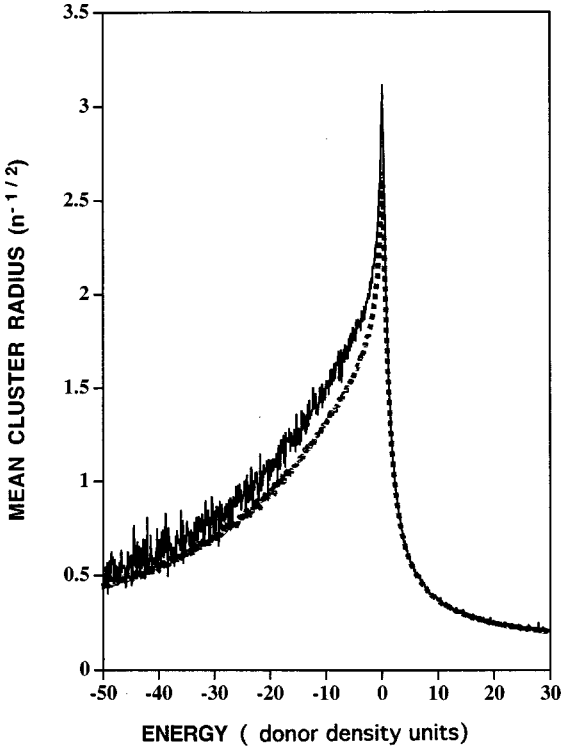

FIG. 4. Variation of mean cluster radius with transition energy in a monolayer of barrier donors. All barrier donors have the same offset. Dashed and solid line curves represent results of calculations for systems with $N=400$ and $N=800$, respectively.

On average, excited-state wave functions with energies close to the unperturbed donor transition energy are associated with relatively spread-out excitations. This is made clear in Fig. 4, where the average excitation radii for eigenfunctions of the Hamiltonian matrix of Eq. (22) are plotted against their associated energy eigenvalues. In that figure a histogram was calculated with an energy bin width of 0.1 and the points representing the ordinates for each bin connected. Calculations for $N=800$ (solid line) are compared to those for $N=400$ (dashed line).

Probability distributions for cluster radii, weighted by the oscillator strength of their associated wave function and normalized to unit area, are shown in Fig. 5, where the abscissa is the ratio of the cluster radius, defined by Eq. (25), to R_{disk}. The histogram defined by the circle symbols represents the overall distribution of excitation cluster radii found in calculations for $N=800$. The connected diamond and square sym-

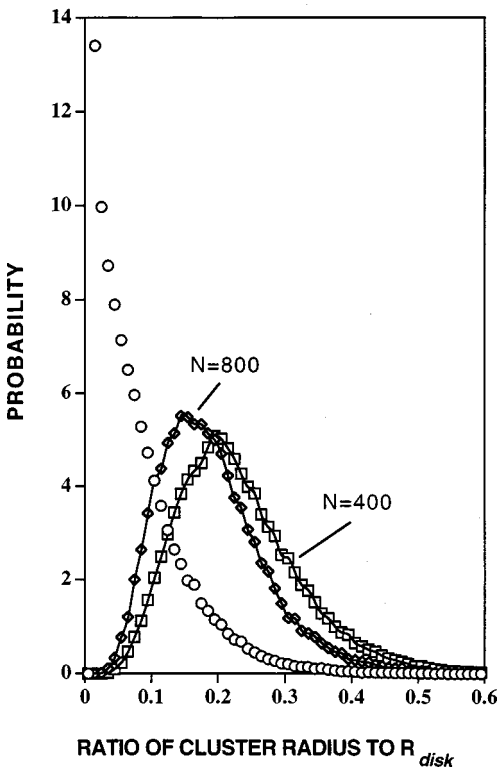

FIG. 5. Probability distributions for finding various cluster radii for barrier donors in a monolayer. The abscissa is the ratio of the cluster radius to the radius of the large disk circumscribing the donor system. The circles represent the distribution for the donor system without regard to the energy of the excitation. The curves represent distributions for excitation energies within 0.1 donor density units from zero. Curves for $N=800$ and $N=400$ are indicated.

bols (for $N=800$ and $N=400$, respectively) represent the distributions of cluster radii for only those eigenvectors with energy (donor density units) lying between -0.1 and $+0.1$. These latter graphs show tails corresponding to very large excitations, suggesting that even at $N=800$ the line-shape calculation may not have completely converged. However, comparison of curves for $N=800$ and $N=400$ in Fig. 5 does support the supposition that excitation cluster radii tend to saturate at sufficiently large N.

IV. LOW-DENSITY LIMIT—MULTILAYERS

The transition energy of an electron bound to a donor ion in the barrier decreases with increasing offset of the donor ion from the x-y plane, as shown in Fig. 1. Substitutional donor ions can lie only in planes in the barrier that occupy a set of offset distances from the x-y plane that are integer multiples of a fixed small distance [one-half of a lattice constant or 0.28 nm in the case of (1,0,0) GaAs wells]. This means that the unperturbed spectrum of donors associated with a number of such planes consists of an equal number of infinitely sharp lines. Because these are separated by energies that do not depend on the concentration of donors the energy separations, when measured in units of $(na^2)^{3/2}R/\gamma$, go to infinity as the density goes to zero. At low but experimentally interesting densities and offset values the energy separations of transitions arising from donors in adjacent layers may be far from negligible. Thus it is not permissible to treat the offset distance as a continuous random variable.

As an example, in our model an isolated donor with an offset of 10 nm from the GaAs quantum well will have a transition energy at $\gamma=1$, which is $0.010R$ greater than the transition energy of a similar donor in the adjacent plane at an offset of 10.28 nm. For a total donor surface density n of $10^{10}/\mathrm{cm}^2$ this amounts to an energy equal to 10 in donor density units. With increasing values of γ this separation remains almost constant, but the linewidths of the peaks decrease, being proportional to γ^{-1}.

We have simulated ''rectangular-doped'' systems in which N_L layers are doped with the same average sheet density per layer of n/N_L. For simplicity we have assumed that the unperturbed transition energies form a comb of equally spaced lines (more realistically, from Fig. 1, the lines crowd together as the offsets of the layers increase). The off-diagonal elements of the Hamiltonian matrix employed in this simulation is the same as in Eq. (22), but the diagonal elements are taken as

$$H_{ii}=-CR_i, \tag{27}$$

where C is the energy spacing between transition energies originating from adjacent layers and R_i is a uniformly distributed random integer in the range 0 to N_L-1. Note that Eq. (27), which assumes a uniform spacing of transition energies, is an approximation valid only if N_L is not too large since, as already mentioned, the spacing of the transition energies actually decreases as the offset distance increases. However, in the present model it is clear that the value of C appropriate for a given offset is approximately proportional to the magnitude of the derivative at that offset of the model curve in Fig. 1. Since this derivative is less than the one predicted from a more realistic calculation the present model appears to underestimate the transition energy spacings.

In Fig. 6 are shown the results of a simulation as described above, for $N_L=8$ and $\gamma=1$ with unperturbed comb spacing equal to 10 donor density energy units. Notice that the lines are well resolved, being far sharper than the monolayer absorption line shape of Fig. 2 at the same value of n.

If we were to attempt to explain the sharpness of the lines in Fig. 6 by a model in which interactions between donors residing in different layers were neglected, we would conclude that with increasing N_L the linewidths, being governed solely by the density of donors in a given layer n/N_L, should shrink like $(n/N_L)^{3/2}$ and should all have line shapes like that of the absorption line shown in Fig. 2. Simulations at various values of N_L show that for large N_L the lines do shrink with increasing N_L but more slowly than predicted from the isolated layer model proposed above. Further, the lines change shape as one progresses from the highest- to lowest-energy line of the comb. It seems clear that for large N_L the interaction between donors in different layers dominates the within-layer interactions. The decrease in linewidth of donors associated with a given layer is a result of the decrease in probability of interactions with donors in nearby layers, which, because they are close in excitation energy, produce relatively large energy shifts, and an increase in probability of interactions with donors with excitation energies far from that of the given layer, producing small energy shifts. (The change in line shape of the lines, depending on their energy

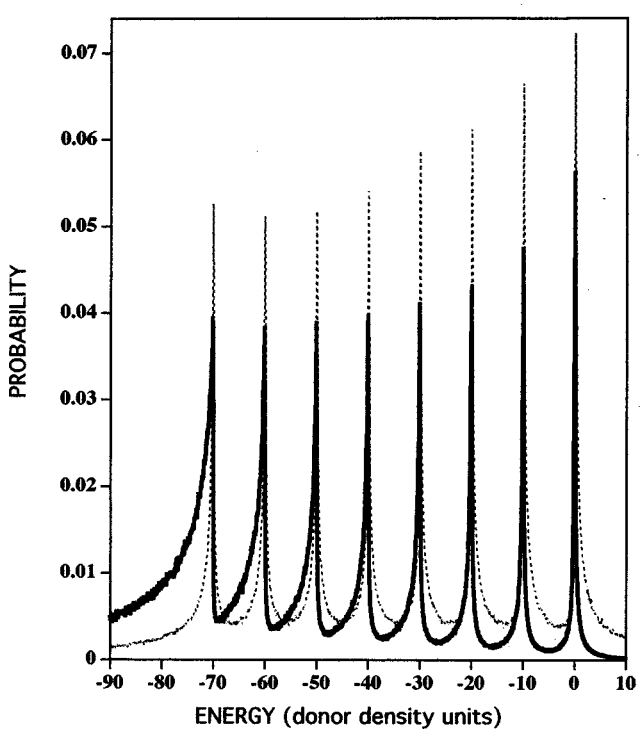

FIG. 6. Predicted absorption line shape (solid line) and unweighted transition energy spectrum (dashed line) for an eight-layer barrier donor system in the extreme low-density limit. Each layer has the same density of donors. Transition energies of isolated barrier donors in adjacent layers are assumed separated by ten donor density units. The zero of energy is the transition energy of an isolated donor in the layer with the smallest offset.

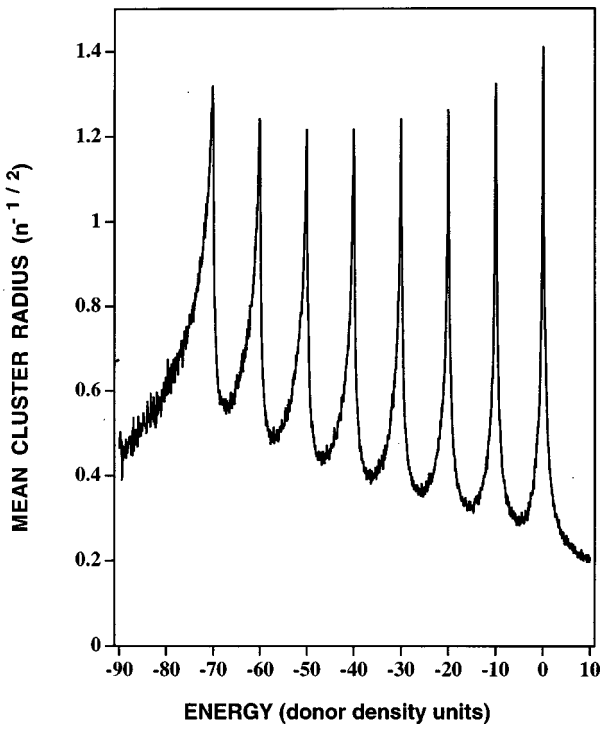

FIG. 7. Variation of mean cluster radius with transition energy in the eight-layer system of Fig. 6.

position in the comb as observed in our simulations at large N_L, is also consistent with the predominant role of interlayer interactions.)

A second interesting feature of Fig. 6 is the close similarity of the transition energy spectrum with the line-shape spectrum, especially in comparison with Fig. 2, where these two spectra are very different. This is connected with the breakup of excitation clusters by the presence of ''diagonal disorder'' associated with the occupation of many layers, an effect that is also reflected in the smallness of the cluster radii, depicted in Fig. 7 for runs with $N=200$. Even near the line peaks the clusters are significantly smaller than the largest found in the monolayer case, Fig. 4. Both of these effects, the coalescence of the line shape and transition energy density spectra and the shrinking of cluster size become more pronounced as N_L increases.

V. HIGHER DENSITIES

We now consider more realistic situations in which (a) the offset values, though small compared to $r_{\rm sep}$, are not completely negligible, and (b) the cyclotron radius r_c is comparable in magnitude to the offset distances. To obtain the spectrum of excitation energies we again take the ground-state energy as zero but now calculate the diagonal matrix elements correct to lowest nonvanishing order in an expansion in inverse powers of the donor separations. Thus we calculate the ith diagonal matrix element for a monolayer by evaluating to this order the term

$$\left\langle \Psi_i \left| \sum_{j=1}^{N} H_C(i,j) \right| \Psi_i \right\rangle - \left\langle \Psi_{\rm GS} \left| \sum_{j=1}^{N} H_C(i,j) \right| \Psi_{\rm GS} \right\rangle, \tag{28}$$

where for $j \neq i$, H_C is defined by Eqs. (11) and (12) and $H_C(i,i)$ is defined to be zero. For multilayer systems the term H_{ii} from Eq. (27) is added to the diagonal element of Eq. (28). In this ansatz, terms representing the Stark effect of electric fields of all the other donors acting on donor i vanish, but the corresponding electric field gradients do affect the line shape. In Appendix A we show that Stark effect perturbations are negligible compared to the terms that we keep.

There are two classes of terms arising from the Taylor expansion of $H_C(i,j)$ that contribute in lowest order to expression (28). These are terms of order $\rho_i^2 d_j^2/s_{ij}^5$ (or equivalently $\rho_j^2 d_i^2/s_{ij}^5$) and those of order $\rho_i^2\rho_j^2/s_{ij}^5$, given in expressions (29) and (31), respectively. These expressions are

$$\{3(\mathbf{s}_{ij}\cdot\boldsymbol{\rho}_j)^2/s_{ij}^5 - \rho_j^2/s_{ij}^3 - [3(\mathbf{s}_{ij}\cdot\boldsymbol{\rho}_j)^2/(s_{ij}^2+d_i^2)^{5/2} - \rho_j^2/(s_{ij}^2+d_i^2)^{3/2}]\} + i\leftrightarrow j, \tag{29}$$

which represents the usual field gradient interaction between the donors and contributes, after angular integration, to expression (28) the term

$$\pi\rho_i^2[1/s_{ij}^3 + (2d_j^2 - s_{ij}^2)/(s_{ij}^2+d_j^2)^{5/2}] \tag{30}$$

and

$$[\{0.75\rho_i^2\rho_j^2+1.5(\boldsymbol{\rho}_i\cdot\boldsymbol{\rho}_j)^2\}/s_{ij}^5-7.5\{(\mathbf{s}_{ij}\cdot\boldsymbol{\rho}_i)^2\rho_j^2+2(\mathbf{s}_{ij}\cdot\boldsymbol{\rho}_i)\times(\mathbf{s}_{ij}\cdot\boldsymbol{\rho}_j)(\boldsymbol{\rho}_i\cdot\boldsymbol{\rho}_j)\}/s_{ij}^7+105(\mathbf{s}_{ij}\cdot\boldsymbol{\rho}_i)^2(\mathbf{s}_{ij}\cdot\boldsymbol{\rho}_j)^2/(4s_{ij}^9)] + i\leftrightarrow j, \tag{31}$$

which, after angular integrations, leads to

$$4.5\rho_i^2\rho_j^2/s_{ij}^5. \tag{32}$$

If terms given in formulas (30) and (32) are inserted into the expression (28), and the integrations performed, one arrives at diagonal terms given in donor atomic units by

$$H_{ii}=\gamma^{-1}\sum_{\substack{j\\ j\neq i}}[1/s_{ij}^3+(2d_j^2-s_{ij}^2)/(s_{ij}^2+d_j^2)^{5/2}+4.5/(\gamma s_{ij}^5)]-CR_i, \tag{33}$$

where we have included the unperturbed donor transition energies in Eq. (33) in the same way as in Eq. (27).

The first correction to the low-density off-diagonal matrix elements given by Eq. (22) is most easily calculated by performing a multipole expansion of the electron-electron repulsion term in $H_C(i,j)$ given in Eq. (11) and retaining the term of order $(s_{ij})^{-5}$. This term is found to be

$$2P_4(\cos\varphi)|\boldsymbol{\rho}_i-\boldsymbol{\rho}_j|^4/s_{ij}^5, \tag{34}$$

where $P_4(\cos\varphi)$ is the fourth-order Legendre polynomial and φ is the angle between $\boldsymbol{\rho}_i-\boldsymbol{\rho}_j$ and $\mathbf{s}_{ij}$. The required matrix element is of the form given by the left-hand side of Eq. (18) with $H_{VW}(i,j)$ replaced by expression (34), and the required integrals are readily calculated if the wave functions are rewritten in relative coordinates. We find the correction to H_{ij} defined in Eq. (22) to be, in donor atomic units,

$$-9/(\gamma^2 s_{ij}^5). \tag{35}$$

In Fig. 8 are shown results employing Eqs. (33), (22), and (35) for a twenty-layer system with smallest offset equal to 20 nm (smallest d value equal to $2a$), areal barrier donor density of 10^{10} donors/cm^2 ($na^2=0.01$), and magnetic field strength of 6.56 T ($\gamma=1$). The comb structure on the curve of predicted absorption line shape (solid line) is easily discerned. Particularly interesting is the comparison of this line with the line shape predicted by neglecting the off-diagonal elements of the Hamiltonian matrix (dashed line). These elements are often neglected in line-shape calculations. The strong shift of the predicted absolute maximum of the absorption peak towards low energy exhibited here may be an important physical effect in observed experimental spectra. It has nothing to do with the crowding together of transitions originating from donors with large offsets (which would further enhance the absoption strength in the low-energy part of the spectrum).

The predicted comb structure is most pronounced for small offsets, high magnetic fields and low doping densities. (We have purposely chosen relatively large offsets and a small magnetic field in Fig. 8 to show that the comb structure persists even in such an ''unfavorable'' circumstance.) So far as we know this structure has not been observed in barrier donor spectra. To observe it would require rather high resolution (in Fig. 8 the comb peaks are separated by about 0.13 cm^{-1}, although at offsets near 10 nm this separation would increase to nearly 0.5 cm^{-1}). Furthermore, the presence of significant concentrations of positive and negative ions in the barrier or well region could broaden out the lines predicted here to the extent that the comb structure could be suppressed and the main peak shifted to higher energies.

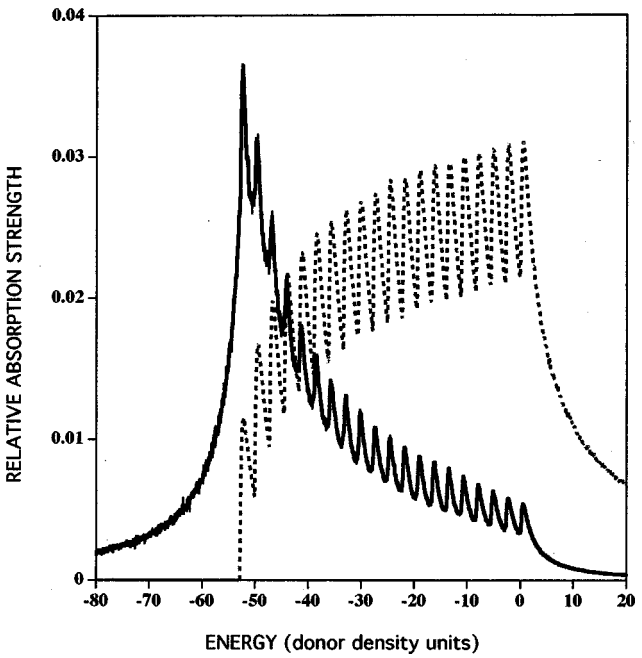

FIG. 8. Predicted line shape of a 20-layer system of barrier donors with equal concentration of donors in each layer (solid line). Density corrections have been applied in the calculations. The dashed curve shows the line predicted if the van der Waals interactions between donors were neglected. The energy separation between transitions of isolated donors in adjacent layers is taken to be 2.78 donor density units, corresponding to $\gamma=1$ and a smallest offset of 20 nm. The zero of energy is the transition energy of an isolated donor in the layer with the smallest offset.

Only those transitions that can arise from the ground state of the donor system have been considered. There are, however many excited levels lying near the ground state that could be thermally populated at low but nonzero temperatures. Transitions from these levels, when superimposed, could in principle wash out the structure predicted here. While our calculation cannot rule out such a possibility, there is reason to think that broadening from thermal population of such levels might be unimportant. In Appendix B we show that at high enough magnetic field, $\gamma d^2\gg 1$, transitions from the low-lying levels mentioned above superimpose exactly on those for the ground state so that thermal excitation of these excited states produces no change in the zero temperature line shape.

VI. CONCLUSIONS

This paper treats absorption line shapes for an idealized system of dilute interacting barrier donors in a single narrow quantum well at zero temperature. The lowest- and next-order terms in the expansion of the absorption energies in powers of the barrier donor density are considered. It is suggested that for densities, fields, and offsets typically utilized

in studies of barrier donor spectra in GaAs-$Al_xGa_{1-x}As$ quantum well structures, it should be possible, in appropriate samples, to resolve transitions arising from substitutional barrier donors at different distances from the center of the well.

APPENDIX A

In donor atomic units (used throughout this appendix) terms of lowest order, γ^{-1}/s^3, and higher order, $\gamma^{-1}d^2/s^5$ and γ^{-2}/s^5, are included in the expansion of the Coulomb potentials between two donors separated by distance s. We have assumed that $\gamma^{-1/2}$ and d are of the same order of magnitude and one order smaller than s. As the surface barrier donor density n decreases the distances s grow in proportion to $n^{-1/2}$. Thus, for example the leading term in the density expansion is of order $n\gamma^{-1}/s$ or, equivalently nr_c^2/s, whereas two higher-energy terms mentioned above are of order $(nr_c^2)(nd^2)/s$ and $(nr_c^2)^2/s$, respectively.

Because of our choice of ground-state basis function, $H_{VW}(i,j)$, given in Eq. (13), has no effect on the ground-state energy. Notice that the ground-state wave function chosen consists of products of functions $\psi_{0,0}$ and that $H_{VW}(i,j)$ connects the unperturbed state $\psi_{0,0}(\rho_i)\psi_{0,0}(\rho_j)$ to $\psi_{0,-1}(\rho_i)\psi_{0,-1}(\rho_j)$; these states have an energy difference of the form $2\gamma^{1/2}f(\gamma^{1/2}d)$. If $f(\gamma^{1/2}d)$ is of order unity then the second-order perturbed energy due to this coupling is of order

$$(1/\gamma s_{ij}^3)^2/[\gamma^{1/2}f(\gamma^{1/2}d)]=O(r_c^5/s_{ij}^6)=(nr_c^2)^{5/2}/r_{\rm sep}, \tag{A1}$$

which is of smaller order than the terms retained. At ultrahigh magnetic fields ($\gamma^{1/2}d\to\infty$) we find that $f(\gamma^{1/2}d)\to 2(\gamma^{1/2}d)^{-3}$ and Eq. (A1) must be replaced by

$$\begin{aligned}(1/\gamma s_{ij}^3)^2/[\gamma^{1/2}f(\gamma^{1/2}d)]&=O(d^3/(\gamma s_{ij}^6))\\&=O((nr_c^2)(nd^2)^{3/2}/r_{\rm sep}).\end{aligned} \tag{A2}$$

A similar argument with similar result holds for the chosen excited state basis functions. Thus it is consistent to ignore $H_{VW}(i,j)$ in second order.

It is easy to show that the electric field component in the x-y plane at a distance s from the barrier donor that produces it, $E(s)$, is of order d^2/s^4. Because of our choice of basis functions these fields give zero first-order contribution to the donor energies. For nondegenerate levels electric fields give rise to a quadratic Stark shift of the donor level. Such electric fields couple, for example, the ground donor state $\psi_{0,0}(\rho_i)$ to the donor level $\psi_{0,-1}(\rho_i)$, which lies above it by an energy $\gamma^{1/2}f(\gamma^{1/2}d)$. The second-order energy in this case is of order

$$\begin{aligned}E(s)^2\gamma^{-1}/[\gamma^{1/2}f(\gamma^{1/2}d)]&=O(\gamma^{-3/2}d^4/s^8)=O(r_c^3d^4/s^8)\\&=O((nr_c^2)^{3/2}(nd^2)^2/r_{\rm sep})\end{aligned} \tag{A3}$$

(assuming d and r_c are comparable in size), which is again of higher order than terms retained. A similar analysis can be applied to the excited state basis functions.[8]

APPENDIX B

In the low-density ultrahigh-field limit, defined by

$$s\gg d\gg r_c,$$

$H_C(i,j)$ can be approximated by expression (29) [expression (31) being neglected because it is of higher order than expression (29) in the ultrahigh-field regime] and the unperturbed barrier donor Hamiltonian takes the expanded form

$$H_{\rm BD}(i)\approx H_0(i)-2/d_i+\rho_i^2/d_i^3. \tag{B1}$$

In this limit the Hamiltonian of the donor system is clearly quadratic in the electron displacements and the energy structure has certain simple features that can be clearly elucidated by introducing the A and B operators of Suzuki and Hensel.[9] These operators, in donor atomic units, are defined for an arbitrary electron j by

$$\begin{aligned}A_j&=[(p_{jx}-\gamma y_j/2)-i(p_{jy}+\gamma x_j/2)]/(2\gamma)^{1/2},\\B_j&=A_j^{\dagger}-i\gamma^{1/2}(x_j+iy_j)/2^{1/2},\end{aligned} \tag{B2}$$

where

$$p_{jx}=\frac{1}{i}\frac{\partial}{\partial x_j},\quad p_{jy}=\frac{1}{i}\frac{\partial}{\partial y_j}.$$

They obey the usual commutation relations for raising and lowering operators

$$[A_j,A_k^{\dagger}]=\delta_{j,k},\quad [B_j,B_k^{\dagger}]=\delta_{j,k} \tag{B3}$$

and every A operator commutes with every B operator (where by A and B operators we always mean A, B, $A^{\dagger}$, and $B^{\dagger}$ operators). The operator A_j lowers both the Landau and M quantum numbers of electron j by one unit. On the other hand, B_j has no effect on the Landau quantum number but raises M by one unit.

Our Hamiltonian is quadratic in the displacements of the electrons from their associated donor centers. Such a Hamiltonian when expressed in A and B operators is a linear combination of products of pairs of these operators. We ignore all terms that can admix states of different Landau quantum numbers N to the unperturbed state of interest. (We neglect such mixing because the energy gap between such levels and the unperturbed level is assumed large compared to the Coulomb energies.) As an example, all terms involving the product of an A operator with a B operator will be omitted.

In this approximation the Landau quantum number N is a good quantum number. The lowest-lying states of the interacting donor system are $N=0$ levels and the optically excited states are $N=1$ levels. Mathematically the eigenstates are product functions of ''A states'' and ''B states'' and the energies are equal to a sum of the energy of the ''A state'' and that of the ''B state.'' We can represent the lowest levels by wave functions of the form

$$|0\rangle_A\theta_B, \tag{B4}$$

where $|0\rangle_A$ is the vacuum state for the A operators, the state such that for all electrons j

$$A_j|0\rangle_A=0, \tag{B5}$$

and θ_B is a particular eigenstate of the B operators in the Hamiltonian. The operator for optical excitation in the dipole approximation is linear in the electronic displacements and therefore in the A and B operators. As a result, when the light excites the system into a state for which $N=1$, the excited state is a product of an excited ''A state'' with the *same* state θ_B as in the initial state. Thus the energy of the excited state is independent of whichever initial state of the form (B4) it arises from.

At high magnetic fields and low temperatures only states of form (B4) are low enough in energy to be thermally populated. As a consequence, if electron-phonon interactions are ignored, the line shapes should be independent of temperature in the ultrahigh field limit at low temperatures.

[1] E. Glaser, B. U. Shanabrook, R. L. Hawking, W. Beard, J.-M. Mercy, B. D. McCombe, and D. Musser, Phys. Rev. B **36**, 8185 (1987).

[2] Y. J. Wang, J. P. Cheng, and B. D. McCombe, J. Electron. Mater. **20**, 71 (1991).

[3] A. Mandray, S. Huant, and B. Etienne, Europhys. Lett. **20**, 181 (1992).

[4] D. M. Larsen, in Proceedings of the 14th International Conference on the Physics of Semiconductors, edited by B. L. H. Wilson [Inst. Phys. Conf. Ser. **43**, 529 (1979)], IOP Conf. Proc. No. 43 (Institute of Physics, London, 1979), p. 529.

[5] D. M. Larsen, Phys. Rev. B **44**, 5629 (1991).

[6] More generally, in cases for which electric forces exerted on electrons with wave functions centered on their respective donor centers cannot be neglected, displacements of the centers of symmetry of the electron wave functions from the donor centers can be calculated self-consistently using Eq. (10). The idea is to find a set of displacements for which classical equilibrium exists ($F=0$ for each electron). Such a treatment may be required when donor offsets are not very small compared to $r_{\rm sep}$ or when compensating impurities are present.

[7] We implicity assume here that the intensity of incident radiation is sufficiently low that at all times the excitation of the donor system remains very small. Then it becomes reasonable to assume, as we have, that to a good approximation we can regard the donor system as being in its ground state for the purpose of calculating absorption probabilities.

[8] Caution must be exercised here since at certain combinations of magnetic fields and offsets the states $\psi_{1,1}(\rho)$ and $\psi_{1,0}(\rho)$ become degenerate. Near this level crossing a separate analysis must be performed. [The wave function $\psi_{1,0}(\rho)$ is given by $\psi_{1,0}(\rho_j)=(\gamma/2\pi)^{1/2}(\gamma\rho_j^2/2-1)\exp(-\gamma\rho_j^2/4)$.]

[9] K. Suzuki and J. C. Hensel, Phys. Rev. B **9**, 4184 (1974), Appendix B.